Architecture Image Studies
AIS Scientific Journal

Vol.6, Issue 4, pp.101-111, 2025
DOI: https://doi.org/10.62754/ais.v6i4.408

https://journals.ap2.pt/index.php/ais/index

Rheometer Quality Inspection System for Smart Factory Based on Deep Learning

Myungsub Lee[1]

Abstract

Quality conformity inspection using rheometer testing is a critical process in the rubber manufacturing industry, particularly for rubber products intended for automotive applications. Traditional methods rely heavily on manual interpretation by skilled experts, which can introduce subjective variability, inefficiencies, and inconsistencies in defect identification. To overcome these limitations, this study proposes an automated inspection system based on deep learning, integrating Long Short-Term Memory (LSTM) networks and Convolutional Neural Networks (CNNs) to capture both temporal and spatial characteristics of rheometer-generated data. Furthermore, material composition information is embedded into both models as auxiliary inputs to provide product-specific contextual information, enabling the system to generalize across various rubber formulations. The proposed method was validated using a dataset of 30,000 samples collected from real industrial processes. Experimental results demonstrate a high level of classification performance, with the ensemble model achieving an average F1-score of 0.9940. These findings confirm that the system offers superior accuracy and robustness in quality assessment tasks, while significantly reducing reliance on manual labor. The proposed solution represents a scalable and reliable approach to smart factory implementation in the rubber manufacturing industry.

Keywords: *Rheometer Testing, Long Short-Term Memory (LSTM), Convolutional Neural Networks (Cnns), Rubber Manufacturing Industry, Quality Conformity Inspection.*

Introduction

The smart factory represents a paradigm shift in modern manufacturing, characterized by the seamless integration of the entire production lifecycle—from product design and development to manufacturing, quality assurance, and distribution—through the application of advanced information and communication technologies (ICTs) [1,2]. This evolution aims to enhance productivity, cost-efficiency, flexibility, and responsiveness to market demands. In recent years, intensifying global competition in the manufacturing sector has driven concerted efforts to bolster industrial competitiveness through technological innovation [3]. These changes have led to the emergence of the Fourth Industrial Revolution, marked by the convergence of digital, physical, and biological systems. In response to this transformation, governments, academic institutions, industry associations, and major enterprises have been actively promoting and investing in smart manufacturing initiatives. Concurrently, global standardization bodies are developing and disseminating reference architectures, technical standards, and interoperable platforms to ensure consistency and scalability across smart factory deployments [4,5]. As a result, the smart factory market has demonstrated consistent annual growth, with a temporary downturn observed only during the global disruption caused by the COVID-19 pandemic. It is projected that this growth trajectory will continue in the coming years, with increasing adoption of emerging technologies such as Artificial Intelligence (AI), Internet of Things (IoT), and blockchain [6–10]. Among these, AI has gained particular attention for its wide applicability in manufacturing processes. Recent studies have explored the use of machine learning and deep learning models for defect detection, predictive maintenance, process optimization, and human-robot collaboration. For instance, AI algorithms enable real-time detection of anomalies in sensor data, simulate manufacturing processes under various conditions, and automate inspection tasks previously reliant on manual labor. Despite global advancements, the adoption of smart factory technologies in some countries remains limited due to legacy infrastructure, insufficient digital maturity, and continued reliance on skilled human resources [11]. In the rubber manufacturing industry, quality control

[1] Yeungnam University College, Daegu, Korea, Email : skydream@ync.ac.kr, ORCID : https://orcid.org/0000-0002-9291-8737

processes such as optimizing compounding ratios and evaluating rheological properties still depend heavily on the empirical experience and intuition of trained technicians. Specifically, rheometer testing—a critical method used to assess the cure characteristics and elasticity of processed rubber—is inherently operator-dependent, leading to variability in outcomes, potential human error, and increased operational costs associated with training and labor [12]. To address these limitations, this study proposes an AI-enabled automated quality inspection system for rubber manufacturing, with a primary focus on rheometer test automation. The proposed framework leverages both time-series and image data to train deep learning models capable of accurately interpreting rheological behavior. Furthermore, the system incorporates the composition of raw rubber materials as auxiliary input features, allowing the model to generalize across diverse rubber formulations. The contributions of this paper are as follows:

- We propose a unified AI model that enables automated rheometer data interpretation across multiple rubber product types by utilizing both sensor data and material composition as multi-modal inputs.
- We introduce preprocessing techniques optimized for time-series and image data to enhance model performance and reliability in a real industrial setting.
- We develop a user interface (UI)-based software prototype that facilitates the practical deployment and validation of the model within existing manufacturing environments.

The proposed system significantly reduces manual workload and operational variability, contributing to the realization of AI-driven smart factory systems in the rubber manufacturing industry. Given the widespread use of rubber products across industries such as automotive, electronics, and construction, ensuring the quality and consistency of these products is of paramount importance. The integration of AI techniques for automated quality assurance not only enhances production efficiency but also ensures safer and more reliable end-use performance. The remainder of this paper is organized as follows. Section 2 provides a review of related research in AI applications for manufacturing and quality inspection. Section 3 details the proposed AI-based model, including data preprocessing strategies, model architecture, and software implementation. Section 4 presents experimental results and performance evaluations. Finally, Section 5 concludes the paper and discusses future research directions.

Related Studies

AI-Based Pattern Detection in Manufacturing

In modern manufacturing environments, the vast volume of data generated by machinery, sensors, and process operations contains a wide array of patterns that can be instrumental in detecting defective products and identifying anomalies in real-time [13]. However, given the diverse range of potential manufacturing scenarios, manually analyzing such data—particularly through visual inspection—presents inherent limitations for non-expert personnel. To address these challenges, a variety of artificial intelligence (AI) techniques have been proposed, enabling automatic pattern recognition and decision-making from complex datasets. In particular, deep learning architectures such as Convolutional Neural Networks (CNNs) and Long Short-Term Memory (LSTM) networks have demonstrated significant efficacy in image and time-series classification tasks, with increasing adoption in industrial applications [14–23].

LSTM networks—designed to capture long-term dependencies in sequential data—are particularly effective for analyzing temporal patterns in time-series or textual data. By learning the temporal structure of input sequences, LSTM models enable accurate forecasting and classification based on dynamic process data. Nevertheless, time-series analysis in industrial settings often involves additional contextual variables that can influence model outcomes. To incorporate such external attributes, advanced variants such as the **Auxiliary LSTM** model have been developed. As illustrated in Figure 3, the Auxiliary LSTM integrates supplementary input data that enhance both model inference and generalization capabilities [15]. This architecture can also be incorporated into CNN-based models, facilitating multi-modal learning. Given that manufacturing data inherently possess both temporal and spatial characteristics, combining CNN and LSTM architectures—with the auxiliary incorporation of production metadata—presents a powerful approach for automated and accurate pattern detection.

Enhancing Industrial Environments Through AI Technologies

Recent studies have illustrated the practicality and effectiveness of integrating deep learning-based AI methods into industrial environments for defect detection and process optimization. Nguyen et al. [16] conducted a comparative analysis of four deep learning models—VGGNet, ResNet, DenseNet, and GoogLeNet—in defect detection tasks using embedded systems. The study reported that DenseNet demonstrated the highest predictive performance, although it required approximately 1.5 times more training time than the other models. Furthermore, the researchers enhanced accuracy by confining model training and inference to selected regions of interest (ROIs) within the image, leading to a performance improvement of approximately 2–3%. Their approach achieved a peak classification accuracy of 99%, validating its applicability for real-time defect detection on production lines.

Song [17] proposed a deep generative model for defect identification in die-casting processes—a domain often constrained by limited labeled data. To overcome these limitations, the author employed two generative modeling techniques: the Variational Autoencoder with Reconstruction along the Projection Pathway (VAE-RaPP), and Fence Generative Adversarial Networks (FenceGAN) [18]. These techniques improved data augmentation and distribution learning, thereby enhancing model robustness under constrained data conditions. Experiments employing three different encoding strategies showed superior performance compared to conventional methods across multiple evaluation metrics.

In another study, Xie et al. [19] applied deep learning and transfer learning techniques to automate the classification of defective agricultural products—specifically carrots. Five CNN-based models were considered (DenseNet-121, ResNet-50, Inception-V3, VGG-16, and VGG-19), with ResNet-50 achieving the highest standalone performance [20]. To further enhance model accuracy, an ensemble model comprising ResNet-50, DenseNet-121, and VGG-16 was constructed, which yielded an F1-score of approximately 97.01%. Moreover, the model achieved a per-image processing time of only 0.09 seconds, demonstrating both efficiency and scalability for real-time quality inspection.

Khorram et al. [21] proposed a hybrid CNN-LSTM architecture (CRNN) designed for bearing fault detection using acceleration sensor data. In their system, CNN layers were first used to extract feature maps, which were subsequently passed to an LSTM network for temporal pattern recognition. The model achieved an impressive accuracy of 99.77%. However, due to class imbalance and limited labeled datasets—a common scenario in plant operations—the authors emphasized the necessity of using Generative Adversarial Networks (GANs) for data augmentation and class balancing.

Spandonidis et al. [22] developed CNN- and LSTM-based models for detecting leaks in industrial pipelines used for oil and gas transportation. In their method, time-series signals from pipeline sensors were transformed into time-frequency spectrograms and analyzed via CNNs, while the LSTM-based Autoencoder (LSTM-AE) model was used to encode raw sensor data for anomaly detection [23]. The system was deployed in a real operational setting at an oil refinery and evaluated over a three-day period, successfully identifying leak events in real time.

Across these studies, a shared theme is the integration of multiple AI models or techniques to enhance defect detection and classification performance. Unlike previous approaches, the method proposed in this study introduces **auxiliary data**—such as material composition and process conditions—into the model architecture. This strategy enables the unified prediction and classification of multiple product types using a single AI framework, offering both scalability and generalizability in real-world manufacturing applications.

Overview of the Proposed Deep Learning-Based System

The architecture of the proposed system is illustrated in Figure 1.

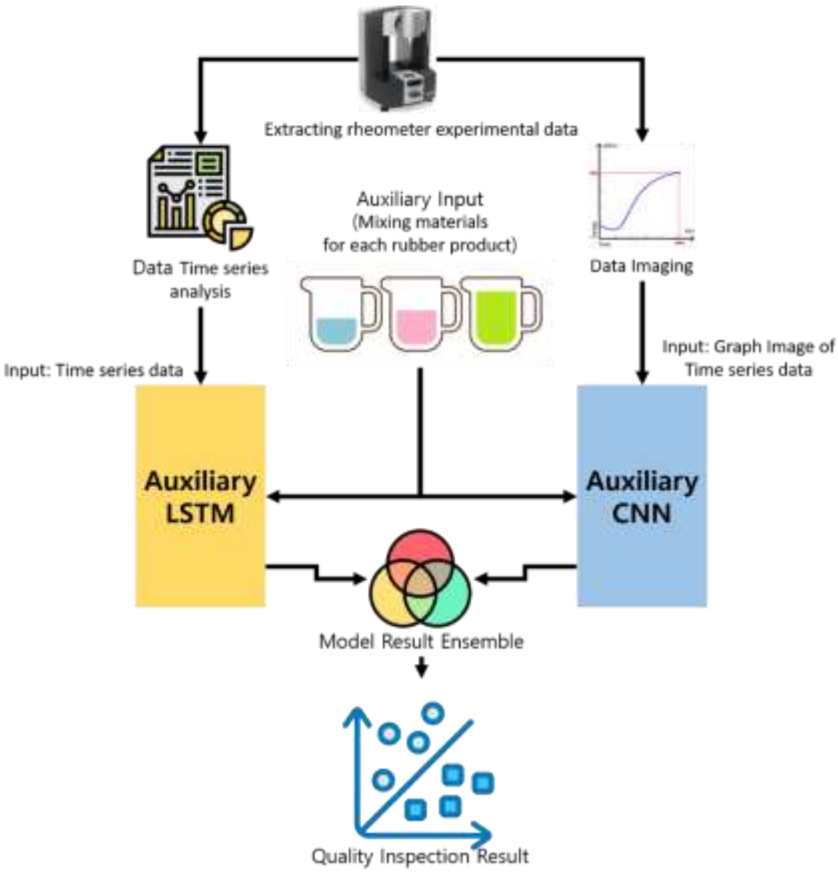

Figure 1. Approach of the Proposed Method

The proposed deep learning-based system for automating rheometer inspections is structured around two primary components: the Auxiliary Convolutional Neural Network (Auxiliary CNN) and the Auxiliary Long Short-Term Memory (Auxiliary LSTM) modules. The overall architecture is designed to leverage multi-modal data—namely, time-series signals and image representations—extracted from rheological measurements of rubber materials. As an initial step, raw rheometer data are systematically preprocessed to extract meaningful patterns while ensuring consistency and scalability. The one-dimensional time-series data, reflecting the viscoelastic properties and cure characteristics captured during rheometer testing, are fed into the Auxiliary LSTM model, which is specifically tailored to process sequential data with temporal dependencies. In parallel, the same rheometer data are transformed into two-dimensional image representations (e.g., plots or spectrograms) that preserve the key visual features of the curing curves. These image data are utilized as input to the Auxiliary CNN, which is optimized for spatial feature extraction. To improve the model's generalization across diverse rubber product types, auxiliary metadata—such as material composition, filler content, or processing parameters—are integrated into both the CNN and LSTM sub-networks. These auxiliary inputs allow the model to account for external factors influencing curing behavior and quality outcomes, thereby enhancing the robustness and applicability of the system across various production scenarios. The outputs inferred from the Auxiliary CNN and Auxiliary LSTM models are subsequently fused using an ensemble learning technique, specifically Soft Voting, to produce the final classification result. This ensemble approach combines probabilistic outputs from both sub-models to determine whether the tested rubber specimen conforms to predefined quality standards. The final decision supports real-time quality assurance processes, thereby reducing dependence on manual inspection and expert judgment.

Auxiliary LSTM Model

The Auxiliary LSTM model is designed to assess the quality conformity of rubber products by learning from sequential patterns in rheometer time-series data, while simultaneously integrating auxiliary information representing the composition of raw and composite materials. The architecture of the proposed Auxiliary LSTM is illustrated in Figure 2.

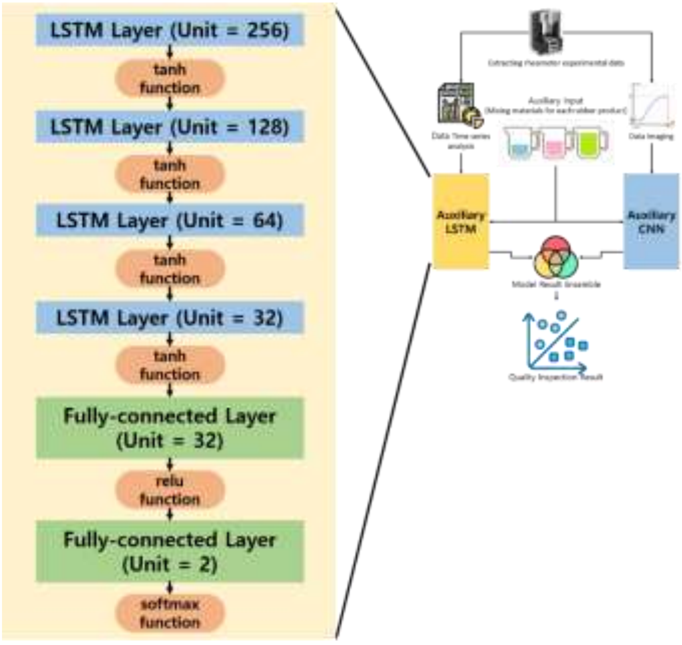

Figure 2. Structure of Auxiliary LSTM used in the Proposed Method

As shown in Figure 2, the network consists of four LSTM layers arranged in a stacked configuration, forming a two-layered architecture. The layers are composed of 256, 128, 64, and 32 memory cells, respectively, each using the hyperbolic tangent (tanh) activation function. This hierarchical structure enables the model to capture both long-term and short-term temporal dependencies inherent in the rheometer measurement curves. Following the LSTM layers, the extracted temporal features are passed to a fully connected (dense) layer to transform the learned information into a representation suitable for classification. At this stage, auxiliary input data—which reflect the characteristics of rubber materials—are integrated into the model. These inputs consist of information detailing the presence or proportion of 32 distinct composite materials used in each rubber formulation. This auxiliary input is concatenated with the LSTM output and fed into another fully connected layer comprising 32 ReLU-activated neurons. Following this, a final output layer with two neurons and a softmax activation function generates a probability distribution over two classes, representing the quality conformity status (i.e., conforming or non-conforming). The binary classification result produced by the Auxiliary LSTM is subsequently combined with the output of the Auxiliary CNN model through an ensemble decision-making mechanism—specifically, Soft Voting—to generate the final inspection outcome.

Auxiliary CNN Model

Conventional neural network structures often rely on one-dimensional input data formats, which can result in the loss of spatial context and local features—particularly when processing image-based inputs derived from manufacturing data. In contrast, Convolutional Neural Networks (CNNs) are well-suited to learn from high-dimensional image representations, as they preserve localized and spatial relationships through convolutional operations. To exploit these advantages, the proposed approach incorporates an Auxiliary CNN model, specifically designed to process image-transformed representations of the rheometer data. The network architecture is illustrated in Figure 3.

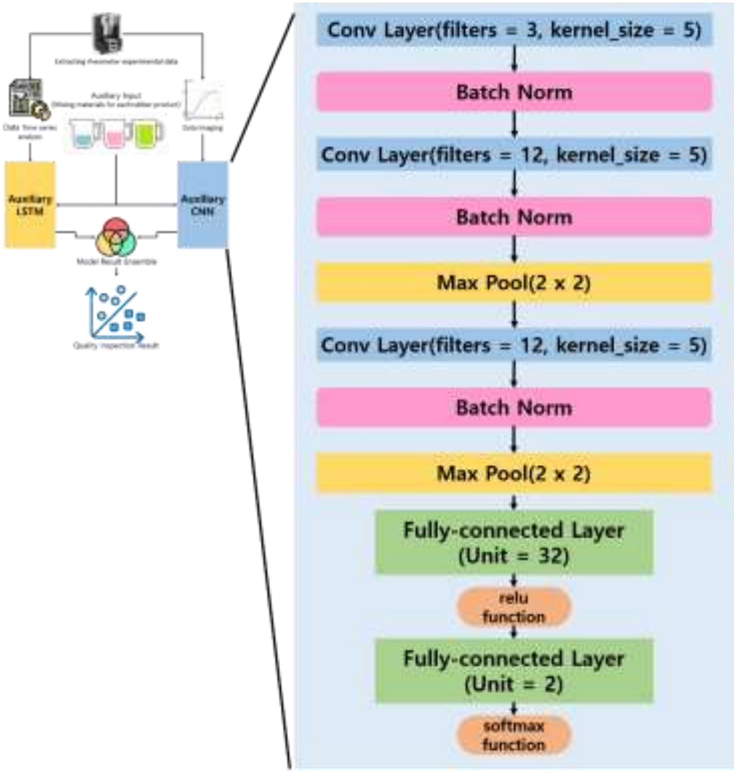

Figure 3. Structure of Auxiliary CNN used in the Proposed Method

As depicted in Figure 3, the CNN model consists of a sequence of convolutional and pooling blocks. Initially, convolutional filters of sizes 3×3 and 12×12 are applied to capture local and global features across different spatial resolutions of the input image. Each convolutional layer is followed by batch normalization, which stabilizes and accelerates the training process by mitigating internal covariate shifts. Subsequently, max pooling layers are employed to reduce the spatial dimensions and to retain the most salient features from each activation map. To further refine feature extraction, an additional convolutional layer with a 12×12 kernel is applied, followed by another set of batch normalization and pooling layers. The resulting high-level feature maps are passed through a fully connected layer, where, similar to the Auxiliary LSTM, auxiliary information related to material composition is included. This combined feature vector then flows into the classification layer, which outputs the binary decision indicating whether the inspected rubber sample meets the predefined quality standards. The predictions from the Auxiliary CNN model are ultimately integrated with the results of the Auxiliary LSTM model through ensemble-based inference, enhancing robustness and overall model reliability in real-world manufacturing conditions.

Data Schema and Representation

Upon completion of rheological testing on a rubber specimen using a rheometer, the raw time-series data and associated metadata are subjected to a preprocessing pipeline before being stored in a structured database. The format of the stored data adheres to the schema presented in Table 1.

Table 1. Schema of Rheometer Time-Series Data

Attribute	*Type*	*Explanation*
rub_code	*text*	*Rubber product code*
create_time	*datetime*	*Process date*
mat_info	*text*	*Material information (Separator: #)*
rheo_info	*text*	*Rheometer measurements (Separator: #)*
result	*int*	*Quality Conformity Inspection Result (1: Acceptance, 0: Defective)*

The schema comprises five attributes: a product identifier (rub_code), a timestamp (create_time) indicating when the rheological test was conducted, binary-encoded material composition data (mat_info), raw sequential measurement data from the rheometer (rheo_info), and a quality inspection label (result). To improve data transparency and storage efficiency, both mat_info and rheo_info are stored as single-line text strings, with the '#' character used as a delimiter to separate consecutive values. Material composition is recorded as a binary vector, where each position denotes the presence (1) or absence (0) of a specific raw or composite material. For instance, a string such as "1#1#0#1" indicates that materials 1, 2, and 4 were included in the formulation. Time-series rheometer data, e.g., "100#102#104#110", represents measurement values taken at 1-second intervals: 100, 102, 104, and 110 at 1s, 2s, 3s, and 4s, respectively. In the proposed system, this structured dataset is utilized by both the Auxiliary LSTM and Auxiliary CNN models, each requiring specific input formatting:

- For the Auxiliary LSTM, the rheometer time-series data are transformed into a fixed-length sequence of 300 measurements, formatted as a one-dimensional vector of shape (1 × 300). This configuration enables efficient temporal pattern recognition while preserving the inherent dynamics of the curing process.

- For the Auxiliary CNN, a graphical representation of the rheometer data is generated and converted into a color image reflecting the cured state. To minimize computational complexity and training time, these images are resized to a format of (1 × 100 × 150 × 3), corresponding to a single RGB image with height 100, width 150, and three color channels. This format is inputted into the CNN to facilitate spatial feature extraction.

Through this schema, the proposed system maintains a standardized database structure that supports scalable training and efficient inference across varying rubber formulations and measurement profiles.

Evaluation

To validate the practical applicability of the proposed system, a comprehensive quantitative evaluation was conducted using a real-world dataset comprising approximately 100,000 samples of raw rheometer time-series data provided by S Corporation, a domestic rubber manufacturing company. The system's performance was evaluated in terms of its ability to classify the quality conformity status of a diverse range of rubber product types. From the full dataset, 70% was allocated for training and 30% for testing. Additionally, a 10-fold cross-validation approach was employed to ensure the robustness and generalizability of the model. All experiments were conducted under consistent environmental settings using TensorFlow 2.0 and Keras for model implementation, and the Scikit-learn library for performance analysis and metric calculation.

Evaluation Metrics and Confusion Matrices

System performance was analyzed using stratified metrics derived from the confusion matrix, namely: precision, recall, accuracy, and F1-score. Table 2 presents the classification results in the form of confusion matrices for the three evaluated models: Auxiliary LSTM, Auxiliary CNN, and the final Ensemble model based on Soft Voting.

Table 2. Confusion Matrix for each Model

Auxiliary LSTM	*Defective prediction*	*Acceptance prediction*	*Sum*
Defective	*11803*	*163*	*11966*
Acceptance	*1048*	*16985*	*18033*
Total sum			*29998*

(a) Auxiliary LSTM

Auxiliary CNN	*Defective prediction*	*Acceptance prediction*	*Sum*
Defective	*11765*	*201*	*11966*
Acceptance	*80*	*17953*	*18033*
Total sum			*29998*

(b) Auxiliary CNN

Ensemble	*Defective prediction*	*Acceptance prediction*	*Sum*

Defective	11873	93	11966
Acceptance	80	17953	18033
Total sum			29998

(c) Ensemble

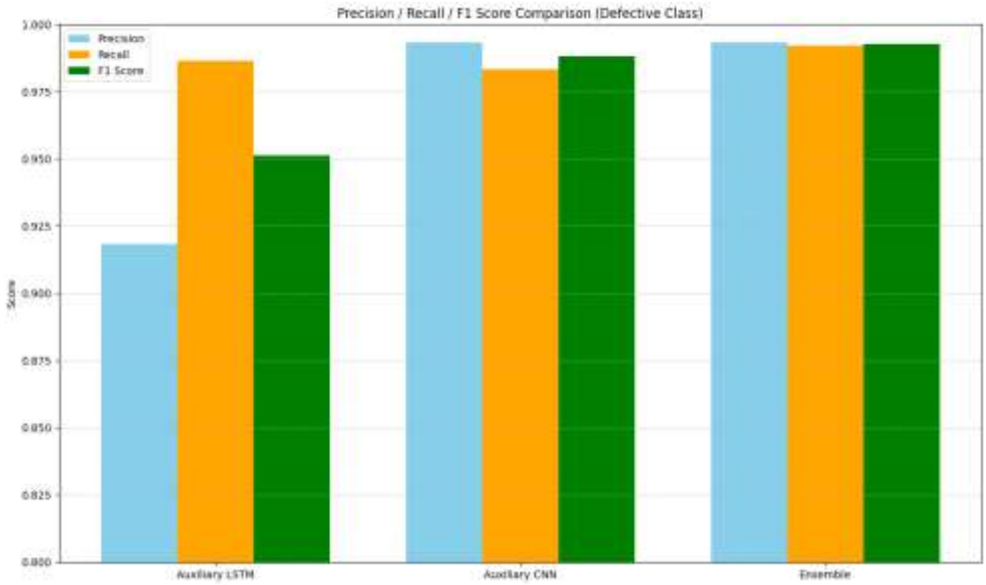

Figure 4. Confusion Matrices For The Three Evaluated Models

As shown in Figure 4, the Ensemble model demonstrates the lowest number of both false positives and false negatives, indicating superior classification performance relative to the standalone Auxiliary LSTM and CNN models.

Performance Comparison by Metric

To further assess classification quality, performance metrics were computed for each class based on the respective confusion matrices. The calculated scores are provided in Table 3, including per-class metrics and macro-averaged values.

Table 3. Classification Performance for each Model

Auxiliary LSTM	Precision	Recall	Accuracy	F1-Score
Defective	0.9185	0.9864		0.9512
Acceptance	0.9905	0.9419	0.9597	0.9656
Average (macro)	0.9545	0.9642		0.9584

(a) Auxiliary LSTM

Auxiliary CNN	Precision	Recall	Accuracy	F1-Score
Defective	0.9932	0.9833		0.9882
Acceptance	0.9890	0.9956	0.9907	0.9923
Average (macro)	0.9911	0.9894		0.9903

(b) Auxiliary CNN

Ensemble	Precision	Recall	Accuracy	F1-Score
Defective	0.9933	0.9923	0.9942	0.9928

Acceptance	*0.9949*	*0.9956*		*0.9952*
Average (macro)	*0.9941*	*0.9939*		*0.9940*

(c) Ensemble

The Auxiliary CNN model demonstrated substantial performance gains over the LSTM model, particularly in terms of precision and recall for the Acceptance class, achieving an F1-score of 0.9923, compared to 0.9656 for the LSTM model. However, for the Defective class, the CNN performance was slightly lower than that of the Ensemble model. The Ensemble model, which aggregates the predictions of both base models using Soft Voting (i.e., the averaging of softmax output probabilities), outperformed both individual models. It achieved an F1-score of 0.9928 for defective cases and 0.9952 for acceptance cases, reaching a macro average F1-score of 0.9940. This indicates that the ensemble strategy effectively leverages the strengths of both models while minimizing their respective weaknesses.

Comparative Model Analysis

Figure 5 provides a visual comparison of the class-wise performance (F1-score) for each model. For both Defective and Acceptance classifications, the Ensemble model displays the highest scores, confirming its robustness across both categories. The consistent improvement across all evaluation metrics demonstrates the effectiveness of the proposed two-branch model architecture and highlights the benefits of incorporating multi-modal inputs and auxiliary data, as well as model fusion techniques, in industrial quality classification tasks.

Figure 5. Class-Wise Performance Comparison of the Three Models

Conclusions

In this study, a deep learning-based quality conformity inspection system for rubber products was proposed, leveraging an ensemble architecture that integrates Auxiliary LSTM and Auxiliary CNN models. By incorporating both rheometer time-series data and material formulation information as auxiliary inputs, the proposed system demonstrated enhanced classification performance and generalizability across multiple types of rubber products. This multi-modal approach enables the model to perform accurate and consistent quality assessments even in the presence of complex input variability. Experimental evaluation using approximately 100,000 real-world samples provided by S Corporation, a domestic rubber manufacturing company, confirmed the system's effectiveness. Across multiple validation trials, the proposed system achieved a macro-averaged F1-score of 0.9940, indicating superior performance in both defect detection and acceptance classification compared to individual deep learning models. The deployment of this system in the operational workflow of S Corporation led to noticeable improvements in inspection speed and accuracy, thereby reducing dependence on manual expertise and minimizing process errors. The proposed approach not only improves operational efficiency but also offers strong potential for scalability and cross-domain applicability. Although the system was developed and tested in the context of rubber manufacturing, the underlying architecture and methodology are expected to be transferable to other industrial applications that involve regular pattern-based quality inspection—such as the evaluation of metallic consumables (e.g., pipes), composite materials, or electronic components. Despite its strengths, the current system is limited by the data imbalance and lack of diversity in the rheometer samples collected from the production site. Most of the training data were associated with a subset of rubber product types, potentially restricting the model's ability to generalize to underrepresented formulations. As a direction for future research, we plan to address this limitation by employing data augmentation techniques, including the use of Generative Adversarial Networks (GANs) to generate realistic and diverse synthetic rheometer data. Furthermore, ongoing work will explore the development of advanced ensemble strategies and transformer-based architectures to further enhance model performance and adaptability. In summary, this study demonstrates that an AI-driven, ensemble-based quality inspection system can serve as an effective tool in smart factory environments, contributing meaningfully to the automation, reliability, and scalability of industrial quality control processes.

Acknowledgment

This research was supported by the Yeungnam University College Research Grants in 2024

References

[1] Precedence Research, "Smart Factory Market Size To Hit USD 321.98 Billion By 2032." [Online]. Available: https://www.precedenceresearch.com/smart-factory-market
[2] M. M. Mabkhot and A. M. Al-Ahmari, "Requirements of the smart factory system: A survey and perspective," Machines, vol. 6, no. 2, p. 23, Jun. 2018, doi: 10.3390/machines6020023.
[3] H. L. Yang and T. W. Choi, "Exploring the research trend of smart factory with topic modeling," Sustainability, vol. 10, no. 8, p. 2779, Aug. 2018, doi: 10.3390/su10082779.
[4] N. Shariatzadeh and T. Lundholm, "Integration of digital factory with smart factory based on Internet of Things," Procedia CIRP, vol. 50, pp. 512–517, Aug. 2016, doi: 10.1016/j.procir.2016.05.050.
[5] B. Chen and J. Wan, "Smart factory of Industry 4.0: Key technologies, application case, and challenges," IEEE Access, vol. 6, pp. 6505–6519, Dec. 2017, doi: 10.1109/ACCESS.2017.2783682.
[6] Bujari and M. Furini, "Standards, security and business models: Key challenges for the IoT scenario," Mobile Networks and Applications, vol. 23, pp. 147–154, Feb. 2018, doi: 10.1007/s11036-017-0835-8.
[7] R. Ozdemir and M. Koc, "A quality control application on a smart factory prototype using deep learning methods," in Proc. 14th IEEE Int. Conf. Computer Sciences and Information Technologies (CSIT), Lviv, Ukraine, 2019, pp. 46–49, doi: 10.1109/STC-CSIT.2019.8929734.
[8] H. T. Nguyen and N. Shin, "Defective product classification system for smart factory based on deep learning," in Proc. 9th Int. Conf. Smart Media and Applications (ICSMA), Jeju, South Korea, Sep. 2020, pp. 80–85, doi: 10.1145/3426020.3426039.
[9] J. Wan and J. Li, "A blockchain-based solution for enhancing security and privacy in smart factory," IEEE Trans. Industrial Informatics, vol. 15, no. 6, pp. 3652–3660, Jan. 2019, doi: 10.1109/TII.2019.2894573.
[10] Y. Zuo, "Making smart manufacturing smarter: A survey on blockchain technology in Industry 4.0," Enterprise Information Systems, vol. 15, no. 10, pp. 1323–1353, Dec. 2020, doi: 10.1080/17517575.2020.1856425.
[11] J. Y. Won and M. J. Park, "Smart factory adoption in small and medium-sized enterprises: Empirical evidence from the manufacturing industry in Korea," Technol. Forecast. Soc. Change, vol. 157, p. 120117, Aug. 2020, doi: 10.1016/j.techfore.2020.120117.
[12] G. Milani and F. Milani, "Rubber blends: Kinetic numerical model by rheometer experimental characterization," J. Math. Chem., vol. 56, pp. 1520–1542, Feb. 2018, doi: 10.1007/s10910-018-0887-4.
[13] Sample and K. Schaffer, "An overview of anomaly detection," IT Prof., vol. 15, no. 1, pp. 8–11, Feb. 2013, doi: 10.1109/MITP.2013.7.
[14] Maschler and T. Knodel, "Towards deep industrial transfer learning for anomaly detection on time series data," in Proc. 26th IEEE Int. Conf. Emerging Technologies and Factory Automation (ETFA), Västerås, Sweden, Sep. 2021, pp. 1–8, doi: 10.1109/ETFA45728.2021.9613542.
[15] H. Liu and J. Wang, "Semi-supervised sentiment classification based on auxiliary task learning," in Nat. Lang. Process. Chin. Comput., Hohhot, China, Aug. 2018, pp. 372–382, doi: 10.1007/978-3-319-99501-4_33.
[16] H. T. Nguyen and G. H. Yu, "Defective product classification system for smart factory based on deep learning," Electronics, vol. 10, no. 7, p. 826, Mar. 2021, doi: 10.3390/electronics10070826.
[17] J. Song and Y. C. Lee, "Deep generative model with time series-image encoding for manufacturing fault detection in die casting process," J. Intell. Manuf., vol. 34, no. 7, pp. 3001–3014, Jul. 2022, doi: 10.1007/s10845-022-01981-6.
[18] P. C. Ngo and A. A. Winarto, "Fence GAN: Towards better anomaly detection," in Proc. 31st IEEE Int. Conf. Tools with Artificial Intelligence (ICTAI), Portland, USA, Feb. 2020, pp. 141–148, doi: 10.1109/ICTAI.2019.00028.

[19] W. Xie and S. Wei, "Recognition of defective carrots based on deep learning and transfer learning," Food Bioprocess Technol., vol. 14, no. 7, pp. 1361–1374, Apr. 2021, doi: 10.1007/s11947-021-02653-8.
[20] B. Koonce, "ResNet 50," in Convolutional Neural Networks with Swift for Tensorflow: Image Recognition and Dataset Categorization, Berkeley, CA: Apress, Jan. 2021, pp. 63–72, doi: 10.1007/978-1-4842-6168-2_6.
A. Khorram and M. Khalooei, "End-to-end CNN+LSTM deep learning approach for bearing fault diagnosis," Appl. Intell., vol. 51, pp. 736–751, Aug. 2020, doi: 10.1007/s10489-020-01859-1.
B. Spandonidis and P. Theodoropoulos, "Evaluation of deep learning approaches for oil & gas pipeline leak detection using wireless sensor networks," Eng. Appl. Artif. Intell., vol. 113, p. 104890, Aug. 2022, doi: 10.1016/j.engappai.2022.104890.
[21] Z. A. Khan and T. Hussain, "Towards efficient electricity forecasting in residential and commercial buildings: A novel hybrid CNN with a LSTM-AE based framework," Sensors, vol. 20, no. 5, p. 1399, Feb. 2020, doi: 10.3390/s20051399.